THE JOURNAL OF PHYSICAL CHEMISTRY B

Article

Development of a Non-Ionic Azobenzene Amphiphile for Remote Photocontrol of a Model Biomembrane

Luciano A. Benedini, Maria Alejandra Sequeira, Maria Laura Fanani, Bruno Maggio, and Veronica I Dodero

J. Phys. Chem. B, **Just Accepted Manuscript** • DOI: 10.1021/acs.jpcb.6b00303 • Publication Date (Web): 12 Apr 2016

Development of a Non-Ionic Azobenzene Amphiphile for Remote Photocontrol of a Model Biomembrane.

Luciano A. Benedini [1] ‡, M. Alejandra Sequeira [1] ‡, Maria Laura Fanani [2], Bruno Maggio [2], Verónica I. Dodero [1] † *.

[1] Instituto de Química del Sur (INQUISUR-CONICET), Departamento de Química, Universidad Nacional del Sur, 8000FTN Bahía Blanca, Argentina.
[2] Centro de Investigaciones en Química Biológica de Córdoba (CIQUIBIC-CONICET), Departamento de Química Biológica, Facultad de Ciencias Químicas, Universidad Nacional del Córdoba, Haya de la Torre y Medina Allende, Ciudad Universitaria, X5000HUA Córdoba, Argentina
*Corresponding author:

ABSTRACT:

We report the synthesis and characterization of a simple non-ionic azoamphiphile, $C_{12}OazoE_3OH$ which behaves as an optically-controlled molecule alone and in a biomembrane-environment. First, Langmuir monolayer and Brewster angle microscopy (BAM) experiments showed that pure $C_{12}OazoE_3OH$ enriched in the (**E**) isomer was able to form solid-like mesophase even at low surface pressure associated with supramolecular organization of the azobenzene derivative at the interface. On the other hand, pure $C_{12}OazoE_3OH$ enriched in the (**Z**) isomer formed a less solid-like monolayer due to the bent geometry around the azobenzene moiety. Second, $C_{12}OazoE_3OH$ is well-mixed in a biological membrane model, Lipoids75^{TM} (up to 20 %mol), and photoisomerization among the lipids proceeded smoothly depending on light conditions. It is proposed that the cross-sectional area of the hydroxyl triethylenglycol head of $C_{12}OazoE_3OH$ inhibits azobenzenes H-aggregation in the model membrane, thus the tails conformation change due to photoisomerization is transferred efficiently to the lipid membrane. We showed that the lipid membrane effectively senses the azobenzene geometrical change photo-modulating some properties, like compressibility modulus, transition temperature and morphology. In addition, photomodulation proceeds with a color change from yellow to orange, providing the possibility to externally monitoring the system. Finally, Gibbs monolayers showed that $C_{12}OazoE_3OH$ is able to penetrate the highly packing biomembrane model, thus $C_{12}OazoE_3OH$ might be used as photoswitchable molecular probe in real systems.

INTRODUCTION:

Molecular self-assembly is the preferred tool of nature to build nano-machines like enzymatic complexes, ribosomes and DNA transcription machinery, biomembranes among others. [1] By simple observation of nature, it is clear that, it is possible to obtain molecular devices with exquisite spatiotemporal control from molecules. This encourages chemists to design new molecules or use nature building blocks like lipids in order to build devices in the nano- and micro-range. [2-4]

In this context, π conjugated building blocks with amphiphilic features are employed because their self-assembly in water is accomplished by thermodynamically driven separation between the polar medium and the rigid π-surface. On the other hand, as π – π interactions are directional such self-assembly can produce structurally precise nano-structures from small molecules.[5.] If the azobenzene moiety is incorporated into an amphiphile structure, the inherent photo-responsive capability of azobenzene group might be transferred to the whole molecule, giving as a result a photo-responsible amphiphilic molecule.[5] Under visible light, the azobenzene adopts its **E** (trans) configuration, and the molecular geometry resembles a rod-type; whereas upon UV-light illumination, the molecular geometry around the azobenzene moiety changes to bent configuration known as **Z** (cis). The change in the length is really important, varying from 9 Å in E configuration to 5 Å in Z configuration.[6] Single-tailed azobenzene amphiphiles are the simplest building blocks to develop photo-tunable chemical systems, often combining guest-host interactions or the presence of lipids.[7-12] The photoswitchable ability is predictable mainly in organic solvent;[13] however, in the aggregate state it will depend strongly on the interaction among molecules. If the azoamphiphile head is ionic in character, the head effective size has a very strong effect on the system packing causing that, if photoisomerization occurs, the molecular geometry change cannot be effectively sensed, especially in mixtures with phospholipids.[14-17] Recently, an ammonium salt head connected to a azobenzene was reported to build up non-phospholipid fluid liposomes with switchable photo-controlled release.[18]

Non-ionic azoamphiphiles are seldom investigated. A successful example was reported based on a azobenzene with simple hydroxyl diethyleneglycol head able to form nano-vesicles which, upon photoisomerization, turned into bicontinuous phase.[19] More recently, other azoamphiphile based on dendritic glycerol head has emerged as suitable building block to obtain photoresponsible spherical micelles.[20, 21] Both systems showed efficient photo-control of the water surface tension.[22, 23] The success of the responsiveness and the resulted functionality were due to the size of the head and the non-ionic character which play an essential role in the packing parameter of both self-assembled systems.

Our general research goals are the application of azoamphiphiles as membrane photo-switches to control spatio-temporarily lipid membranes and cells. In this context, Langmuir and Gibbs monolayers have offered great potential for the study of the organization of soft amphiphilic materials[24] and in particular of lipids to understand the packing of molecules based on their chemical structure, intermolecular interactions, and interactions with the supporting subphase.[25-27] In fact, Langmuir monolayers have been used to model azobenzenes self-assembly at the interface and processes occurring within them.[28-30] However, their use to evaluate the behavior of azobenzene/lipids mixtures was not reported.

The aim of the present work is to present a simple non-ionic photoswichtable azoamphiphile, 4-dodecyloxi-4'-(1-hydroxy triethylenglycol) azobenzene ($C_{12}OazoE_3OH$) which behaves as photo-switchable probe alone and when it is mixed with a biological membrane mimetic, Lipoids 75™. The photoisomerization of $C_{12}OazoE_3OH$ among the lipids induces interfacial, morphological and thermal changes of the biomimetic membrane. Importantly, we showed that $C_{12}OazoE_3OH$ is not only well mixed in the biomembrane, but also it is able to penetrate it from the subphase. Altogether, our findings show that $C_{12}OazoE_3OH$ might be an efficient photo-responsible probe to remote control of biological membrane properties.

EXPERIMENTAL SECTION

Material and Synthesis:

All manipulations were carried out under an atmosphere of nitrogen. Acetonitrile was dried over K_2CO_3 and distilled immediately before use.

1-dodecyloxi-4-nitrobenzeno **(1)**: To a solution containing 886.3 mg (6.38 mmol) of nitrophenol and 5.28 g (38.28 mmol) K_2CO_3 in 20 ml acetonitrile under stirring was added 1.85 ml (7.66 mmol) dodecyl bromide in 10 ml acetonitrile. The reaction mixture was refluxed for 27 hours and subsequently filtered through Celite. The solvent was removed by reduced pressure and the crude product was obtained as a solid. This solid was further purified by column chromatography on neutral aluminum oxide (hexane: diethyl ether) and **1** was recovered as a white solid in 90% yield. ^{1}H NMR ($CDCl_3$, 300 MHz) δ (ppm): 0.88 (t, 3H, J^3= 6.9 Hz, CH_3), 1.27-1.47(m, 18H, CH_2), 1.82 (m, 2H, CH_2), 4.05 (t, 2H, J^3= 6.0 Hz, OCH_2), 6.93 (d, 2H, J^3= 9.0 Hz, Ar-H), 8.19 (d, 2H, J^3= 9.0 Hz, Ar-H). ^{13}C-NMR ($CDCl_3$) δ (ppm): 14.07 (CH_3), 22.67, 25.91, 28.98, 29.29, 29.32, 29.52, 29.56, 29.62, 29.63, 31.91 (CH_2), 68.93 (OCH_2), 114.41, 125.8, 141.4, 164.26 (Ar-C).

4-dodecyloxi-aniline **(2):** To a solution of 300.0 mg (0.98 mmol) 1-dodecyloxy-4-nitrobenzeno (**1**) dissolved in 10 ml anhydrous $CHCl_3$ was added 8.6 ml methanol. The reaction was stirred in the presence of 50.0 mg of 10% Pd/C under hydrogen atmosphere for 4-6 hours at room temperature. Then, it was filtered off and the solvent was removed under reduced pressure with quantitative yield. The bright grey solid (**2**) was used without further purification in the following step.

4-dodecyloxy-4'-hydroxyl azobenzene (**3**): To 271.5 mg (0.98 mmol) of (**2)** in 4.50 ml of 1:1 aqueous acetone was added 0.45 ml of hydrochloric acid concentrated. To this mixture 2.25 mL of aqueous $NaNO_2$ (93.15 mg, 1.35 mmol) was added and the solution was maintained at 0ºC for 1 h. The resulting diazonium slurry was then added to the following mixture: phenol 131.6 mg (1.40 mmol), NaOH 52.9 mg (1.32 mmol), Na_2CO_3 229.0 mg (2.16 mmol) in 3.80 ml of MilliQ water maintaining the temperature at 0ºC for an additional 1 h. Then, the mixture was stirred for further 16 h at room temperature. After this, it was neutralized with acetic acid and the precipitate containing compound (**3)** was well washed with MilliQ water. Further purification was not necessary, 40% yield (mp 96-97 ºC). ^{1}H NMR ($CDCl_3$, 300 MHz) δ (ppm): 0.88 (t, 3H, J^3= 6.9 Hz, CH_3), 1.27-1.47 (m, 18H, CH_2), 1.81 (m, 2H, CH_2), 4.03 (t, 2H, J^3= 6.0 Hz, OCH_2), 4.63 (s, 1H, OH), 6.93 (d, 2H, J^3 = 9 Hz, Ar-H), 6.98 (d, 2H, J^3 = 9 Hz, Ar-H), 7.81 (d, 2H, J^3 = 9 Hz, Ar-H), 7.85 (d, 2H, J^3 = 9 Hz, Ar-H). ^{13}C-NMR ($CDCl_3$) δ (ppm): 14.07 (CH3), 22.67, 26.025, 29.22, 29.33, 29.38, 29.56, 29.58, 29.62, 29.65, 31.91 (CH2), 68.40 (OCH2), 114.72, 115.76, 124.33, 124.51, 146.91, 147.23, 161.27 (Ar-C).

4-dodecyloxi-4'-(1-hydroxy triethylenglycol) azobenzene **(4)**: To 75.0 mg (0.197 mmol) of 4-dodecyloxy-4'-hydroxyl azobenzene (**3**) and 300 mg (2.17 mmol) K_2CO_3 suspension was added 63.0 mg (0.207 mmol) triethylene glycol p-toluenesulfonate in 10 mL of dry acetonitrile The reaction mixture was allowed to react at reflux for 80 hours and then filtered out. The solid was further purified by column chromatography on neutral aluminum oxide (hexane: diethyl ether) and pure (**4)** in 55% yield was obtained. $C_{12}OazoE_3OH$ shows thermotropic behaivor: Cr-SmC at 91.67°C (ΔH= 88.10 J g^{-1}) SmC-PI at 107.28 °C (ΔH= 33.77 J g^{-1}). The LC behavior is not described here.
^{1}H NMR (400 MHz; $CDCl_3$): δ (ppm)= 0.88 (t, 3H, J^3= 6.9 Hz, CH_3), 1.27-1.47 (m, 18H, CH_2), 1.81 (m, 2H, CH_2), 2, 08 (s, 1H-, OH); 3,61-3,74 (m, 8H, CH_2); 3,90 (t, 2H, J^3= 6.0 Hz, OCH_2); 4.03 (t, 2H, J^3= 6.0 Hz, CH_2), 4,22 (t, 2H, J^3= 6.0 Hz, CH2); 6.99 (d, 2H, J^3 = 9 Hz, Ar-H), 7.00 (d, 2H, J^3 = 9 Hz, Ar-H), 7.86 (d, 2H, J^3 = 9 Hz, Ar-H), 7.87 (d, 2H, J^3 = 9 Hz, Ar-H). ^{13}C-NMR ($CDCl_3$): δ (ppm) = 14.10 (CH_3), 22.68, 26.00, 29.22, 29.33, 29.40, 29.50, 29.60, 29.63, 29.65, 31.91 (CH_2), 61.8, 69.15, 69.71, 70.45, 70.59, 70.90, 72.50 (OCH_2), 114.71, 114.85, 124.26, 124.32, 146.97, 147.32, 160.65, 161.275 (Ar-C). EM-FAB: (m/z): 515, 40 ($M+1H^+$) EMAR: calculated for $C_{30}H_{46}N_2O_5$ 515, 34 found. 515, 35.

Synthesis of Vesicular Membranes

Lipoid s75^{TM} containing 69-75% phosphatidylcholine was purchased from Lipoid Co. (Germany). Other constituents of Lipoid s75^{TM} are: 9.8% phosphatidylethanolamine and 2.1%, lysophosphatidylcholine and had a fatty acid composition of palmitic (17%–20%), stearic (2%–5%), oleic (8%–12%), linoleic (58%–65%) and linolenic (4%–6%) acid. [31] Chloroform was HPLC grade. Water was purified by using a Milli-Q (Millipore, Billerica, MA) system, giving a product with a resistivity of ~ 18.5 MΩ/cm.

Mixtures of $C_{12}OazoE_3OH$: Lipoid s75 ^{TM} were conducted following the technique for obtaining a thin film. The procedure involves the formation of a homogeneous organic film by vacuum evaporation at room temperature of a chloroform solution of the $C_{12}OazoE_3OH$ amphiphile (Z-E: 5-95, 20 mol %) exposed to white light and Lipoid s75^{TM} (80 mol %). To hydrate the film, Milli-Q water at the lipid transition temperature (55ºC) is added to the round bottom flask, under slow rotatory movement for 2 hrs. The next process involves vigorous shaking using a vortex, and then

sonication of the sample to obtain the suspension of the film. Finally it is necessary at least two days aging to achieve formation of the vesicular membranes, multilayers (approximately 0.5 mM). The same procedure was performed to form pure Lipoid s75™ vesicular membranes.

Methods:

UV-Vis Spectroscopy: Switching experiments were done with an 8 watts mercury arc lamp with filter of 360 nm from Pleuger Antwerp Brussels and a white light bulb of 60 watts. UV-Vis spectroscopy data were recorded on a JASCO V-630BIO Spectrophotometer equipped with an EHCS-760 peltier.

Surface Pressure-Area Isotherms of Langmuir Monolayers: The first compression isotherms at 24 °C and 13 °C were performed for both $C_{12}OazoE_3OH$ (4) and $C_{12}OazoOH$ (3) compounds. These compounds were dissolved in a methanol/ chloroform (2:1) mixture to obtain a solution of 1 mg/ml total concentration which was spread onto a 266 cm^2 Teflon trough filled with 200 ml of subphase. Concentration of 1 mg/ml of a mixture of Lipoid s75™. The same protocol were used for mixed monolayers of Lipoid s75™: $C_{12}OazoE_3OH$ (4) (80:20 mol%). The aqueous solution used as the subphase was pH ~ 5.5 (NaCl 145 mM) for all the monolayer experiments. The film was allowed to stand 5 min for solvent evaporation and monolayer relaxation at < 0.1 mN/m before being subsequently compressed isometrically at a compression rate of 2 ± 1 $Å^2$ $molecule^{-1}$ min^{-1}.

The surface pressure was determined with a Pt plate using the Wilhelmy method, and the film total area was continuously measured and recorded using a KSV Minitrough apparatus (KSV, Helsinski, Finland) enclosed in an acrylic box which was continuously enriched with N_2 gas in order to prevent lipid oxidation. The subphase temperature (±0.5 ºC) was controlled by an external circulation bath and kept at 25 ºC, unless indicated.

A representative experiment is shown in all figures from a set of three independent experiments that differed in mean molecular area (MMA) and surface pressure measurements by less than 2 $Å^2$ and

0.2 mN/m, respectively. In order to analyze the film elastic behavior of the adsorbed molecules, the compressibility modulus Cs^{-1} was calculated from the isotherm data as, [32]

$$C_s^{-1} = -MMA\left(d\pi / dMMA\right)_T$$

where π represents the surface pressure. Measurements were carried out in darkness for $C_{12}OazoE_3OH$ **(Z)**.

Brewster Angle Microscopy (BAM) Measurements: Monolayers of $C_{12}OazoE_3OH$ **(E)**, **(Z)** and $C_{12}OazoOH$ **(E)** were prepared as described above using a KSV Minitrough apparatus (KSV, Helsinski, Finland). The Langmuir apparatus was mounted on the stage of a Nanofilm EP3 imaging elipsometer (Accurion, Goettingen, Germany) used in the BAM mode. Zero reflection was set with a polarized 532 λ laser incident on the bare aqueous surfaces at the experimentally calibrated Brewster angle (~53.1º). After monolayer formation and compression, the reflected light was collected with a 20X objective. Under the required calibration, the gray level of each pixel of the BAM images is directly related to the square of the film thickness and refraction index, in films that do not show optical activity; [33] otherwise, the gray level also depends on the orientation of the 2D crystal.

Adsorption of Azo-amphiphiles to Bare Air/Water Interface: Gibbs Monolayers. After injection of 25 µl of $C_{12}OazoE_3OH$ (**E**) or 50 µl of $C_{12}OazoE_3OH$ (**Z**) to the aqueous subphase of a Teflon trough under continuous stirring (trough volume: 15 ml; final subphase concentration 3.2 µM for $C_{12}OazoE_3OH$ **(E)** and 6.39 µM for $C_{12}OazoE_3OH$ **(Z)**, the changes in surface pressure and surface potential at constant area were registered as a function of time, while a Gibbs monolayer was established. Surface pressure was determined as described above. The equipment used was a homemade circular Langmuir balance controlled by an electronic unit (Monofilmetter). All experiments were performed at 23 ± 2 °C. Measurements were carried out in darkness for $C_{12}OazoE_3OH$ **(Z)**.

Penetration of Azo-amphiphiles to Phospholipid Monolayers: Penetration time curves were performed by deposition of a chloroform solution of Lipoid s75™ at the air/water interface, in order to form a monolayer previous to the injection of $C_{12}OazoE_3OH$ (25µL of (Z) and 50 µL of (Z)) in the subphase. Measurements were carried out in darkness for $C_{12}OazoE_3OH$ **(Z).**

Differential Scanning Calorimetry (DSC): Calorimetric measurements were performed with a Q20 Differential Scanning Calorimeter (TA Instruments). Samples were prepared using closed hermetic aluminum pans which had been weighted with a ± 0.00001 g precision balance adding 10 mg of the corresponding compound or water dispersion (2.8 mg/ml) to the pan: a) $C_{12}OazoE_3OH$ **(E)** solid, b) Lipoid s75™ multilamellar vesicular dispersion alone c) Mixtures of Lipoid s75 ™: $C_{12}OazoE_3OH$ **(E)** multilamellar vesicular dispersion and d) Mixtures of Lipoid s75 ™: $C_{12}OazoE_3OH$ **(Z)** multilamellar vesicular dispersion obtained by irradiating the Lipoid s75 ™: $C_{12}OazoE_3OH$ **(E)** for 40 minutes with UV light (360 nm, 8 watts). The same procedure was performed to Lipoid s75 ™ vesicular membranes alone, showing no significant physical changes. The calorimetric measurements were performed at a rate of 5°C/min.

Polarized Optical Microscopy (POM): A drop of the corresponding dispersion of 2.8 mg/ml concentration was placed on glass and cover. POM were performed at 25°C using a Nikon Eclipse E200 POL polarizing microscope.

RESULTS and DISCUSSION

Design, Synthesis and Photoisomerization. Regarding to potential applications, we designed a structural simple amphiphile, $C_{12}OazoE_3OH$ (**4**), by a simple and versatile methodology (Scheme 1). $C_{12}OazoE_3OH$ was obtained directly from commercial 4-nitrophenol in four steps, with an overall yield of 86 %. The introduction of oxygen atoms as connectors between the azobenzene moiety and the head and tail is synthetically simple and allows efficient photoisomerization with slow thermal back-isomerization. Based on previous reports, [19-22] we hypothesized that the hydroxyl

triethylenglycol head would increase the effective cross section area, thus favoring the molecular motion of the tails in the aggregate due to light illumination. Finally, the incorporation of a C12 hydrophobic tail will favor bilayer formation and potential good mixing with natural lipids in biological membranes.[34]

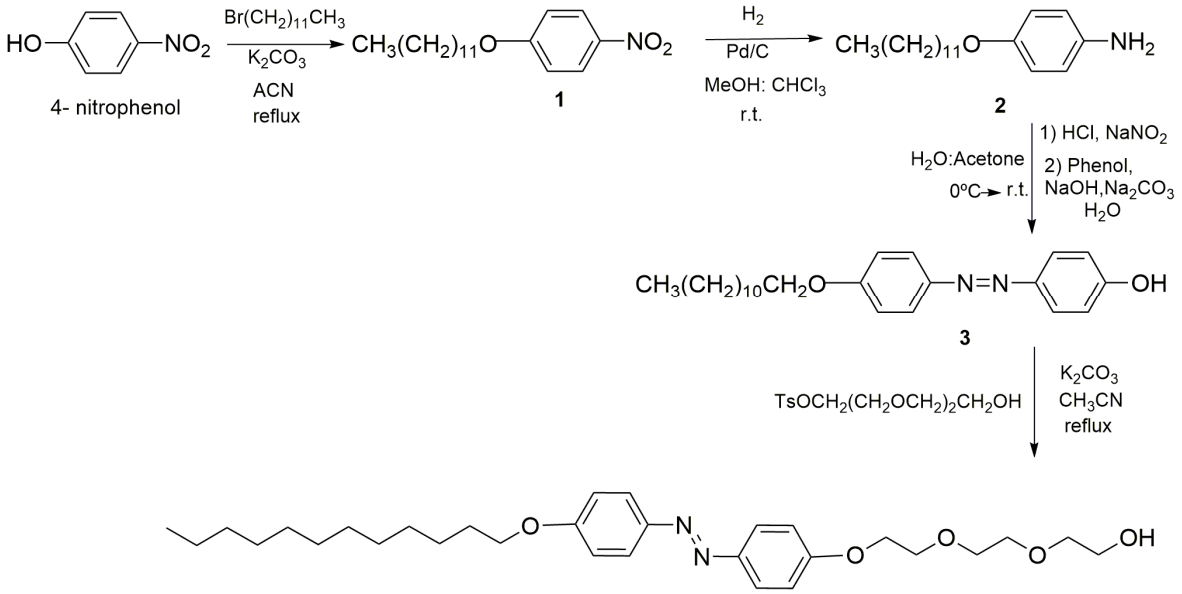

Scheme 1: Synthetic pathway to $C_{12}OazoE_3OH$ **(4)**.

In chloroform, $C_{12}OazoE_3OH$ **(4)** is a yellow solution composed of isomeric mixture of E: Z (95:5) determinated by ^{1}H-RMN which is named for simplicity as $C_{12}OazoE_3OH$ (**E**) (see ESI). Upon UV-light illumination (360 nm, 8watts, 1 min) a photostationary state (pss) of E: Z (10:90) is reached, named as $C_{12}OazoE_3OH$ (**Z**) (orange solution). The photoconvertion ratio from E to Z isomer was evident from ^{1}H-RMN experiments and UV-Vis spectra (Figure 1). UV-Vis spectrum of $C_{12}OazoE_3OH$ (**E**) showed a characteristic π- π* transition centered in 358 nm and a small band at 450 nm corresponding to n- π* transition. The Z→E isomerization was accelerated by illumination with ordinary white light bulb of 60 watts (λ > 445 nm, 3 h, see ESI). The new π- π* transition was blueshifted to 311 nm and the band corresponding to n- π* transition at 450 nm was more evident. Thermal Z→E isomerization is slow enough allowing the evaluation of both pss separately (stable

18 h in darkness). This experiment suggests that $C_{12}OazoE_3OH$ could be used as optically controlled probe.

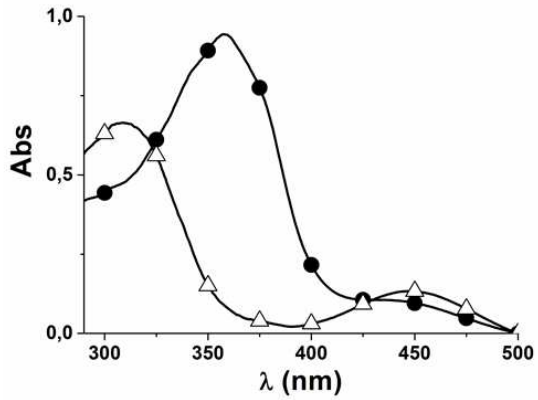

Figure 1. UV-Vis spectra of $C_{12}OazoE_3OH$ before (●) and after (△) UV-light illumination in chloroform (7, 5 μM). Optical stability was achieved up to five cycles.

Langmuir Monolayers. First compression curves of Langmuir monolayers at 24 °C shown in **Figure 2a** exhibited higher values of collapse pressure for $C_{12}OazoE_3OH$ **(E)** (~53mN/m) than $C_{12}OazoE_3OH$ **(Z)** (42 mN/m). The mean molecular area (MMA) at such high pressures for both $C_{12}OazoE_3OH$ **(E)** and $C_{12}OazoE_3OH$ **(Z)** are similar (~23 ± 2 $Å^2$/molecule), showing that the azobenzene group is perpendicular to the surface plane at collapse pressure.[35] This value is in agreement with those reported previously [22] for a compound with a hydroxyl diethylenglycol head and different linkers between the azo moiety and the hydroxyl head, (C_4azoO<u>Linker</u>E_2OH). Moreover, it is close to the cross-section area of hydrocarbon chain ~18 $Å^2$/molecule. [32]

The compression isotherms of compound **3** $C_{12}OazoOH$ **(E)** (E: Z (90:10)) were included to compare the influence of the head length. Both $C_{12}OazoE_3OH$ **(E)** (▲) and $C_{12}OazoOH$ **(E)** (●) monolayers were similar in saline solution pH_b~ 5.5, showing a phase transition at low surface pressure ($\pi \leq 5$ mN/ m) and a collapse at ~ 55 and 60 mN/ m, respectively. However, $C_{12}OazoOH$ **(E)** monolayers showed no sign of a pressure decrease after collapse, showing high stability of the film at 24 °C (not shown). This effect has been reported previously in monolayers of azobenzene-

polyvinyl alcohol and for urea-azobenzene derivatives [35] and it was associated with strong intermolecular interactions. Here, the π-π stacking of the aromatic rings of C_{12}OazoOH **(E)** may be maximal due to the minor steric repulsion of the small OH head. The phase transition of C_{12}OazoE_3OH **(E)** occurred at 50 $Å^2$/molecules, whereas for C_{12}OazoOH **(E)** it occurred at 40 $Å^2$/molecules. In this case, the larger hydroxyl triethylenglycol group in C_{12}OazoE_3OH **(E)** had to exert stronger head group repulsion than the hydroxyl head in C_{12}OazoOH **(E)**, resulting in a higher MMA when phase transition occurs. C_{12}OazoOH **(3)** showed a fast thermal Z-E isomerization rate after UV illumination, thus the Z enriched pss was not measured at the air/water interface. Langmuir monolayer compression curves of C_{12}OazoE_3OH **(Z)** showed a smooth slope with no transition until the collapse. The bent geometry around the azobenzenes of C_{12}OazoE_3OH **(Z)** could be the reason of such behavior. Similar results for *E* and *Z* isomers were described previously for other azobenzenes amphiphiles and it was explained considering supramolecular organization at the air/water interface.[36, 37]

For C_{12}OazoE_3OH (E), C_{12}OazoE_3OH (Z) and C_{12}OazoOH (E) films, the solubility into the subphase was evaluated by assessing the rate of monolayer area loss when kept at the constant surface pressure of 35 mN/m (ESI, Fig. S7). The films composed by C_{12}OazoE_3OH (E) and C_{12}OazoOH (E) show a rate of area loss of 13 % and 5% after 23 min, respectively, being aprox. 28% for C_{12}OazoE_3OH (Z) monolayers. This experiment evidenced a higher solubility of the isomer (Z) at a constant high constant pressure compared with the (E) isomers, which can be explained by the increase of dipole moment of the Z isomer. [6]

Monolayer curves of C_{12}OazoE_3OH **(E)** at 13 °C displayed essentially the same collapse characteristics (MMA and surface pressure) than those at 24 °C; however, at 13 °C the phase transition at 50 $Å^2$/molecule was not observed (ESI, Fig. 6). Nevertheless, the monolayers at 13 °C were more suitable for BAM experiments due to their reproducibility.

The C_{12}OazoOH **(E)** film shows a condensed or solid character as evidenced by a relatively high Cs^{-1} values (300 mN/m, Figure 2b)**,** above 5 mN/m.[37] For C_{12}OazoE$_3$OH **(E)** monolayers, it was observed a less compact behavior with Cs^{-1} ~ 100 mN/m, suggesting LC state at π > 5 mN/m. The difference of Cs^{-1} values between C_{12}OazoE$_3$OH **(E)** and C_{12}OazoOH **(E)** reinforces the idea that C_{12}OazoOH **(E)** forms highly condensed monolayers due to strong intermolecular interaction which did not operate neither in C_{12}OazoE$_3$OH **(E)** monolayers nor in the monolayers of C_{12}OazoE$_3$OH **(Z) (**Cs^{-1} ~60 mN/m).

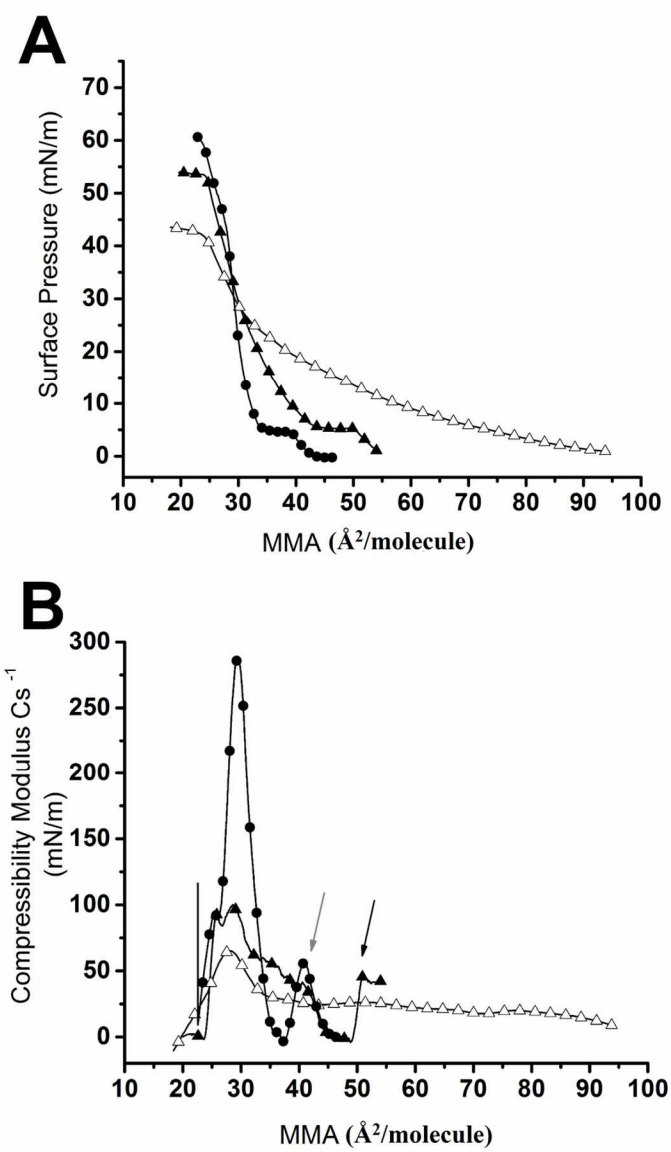

Figure 2. A) Langmuir isotherms at 24°C, compression rate of 2±1 $Å^2$ $mol^{-1}min^{-1}$: $C_{12}OazoE_3OH$ (**E**) (▲), $C_{12}OazoE_3OH$ (**Z**) (△) and $C_{12}OazoOH$ (**E**) (●). **B)** Compressibility modulus of $C_{12}OazoE_3OH$ (**E**) (▲), $C_{12}OazoE_3OH$ (**Z**) (△) and $C_{12}OazoOH$ (**E**) (●). Arrows indicate the beginning of the phase transition. The curves shown are chosen from a set of duplicates that differed by less than 2 $Å^2$/molecule.

Brewster Angle Microscopy. **Figure 3A** shows that $C_{12}OazoOH$ **(E)** displays a solid-like character, detecting positive spherulites at low surface pressure (<1 mN/m) characteristic of a Hexatic I mesophase [38] which it was lost above 5 mN/m. On the other hand, $C_{12}OazoE_3OH$ **(E)** and $C_{12}OazoE_3OH$ (**Z**) monolayers are composed of highly reflective and micro-heterogeneous phases, which resemble a condensed phase. Pedrosa et. al. [37] described the same behavior for a carboxylic azobenzene derivative, they attributed the features to the tendency of E azobenzene hydrophobic tails to form face to face H- aggregates at the air/water interface. In particular, $C_{12}OazoE_3OH$ **(E)** shows below 3 mN/m islands of expanded phase which further increase of the surface pressure lead to a uniform solid-like mesophase similar to those observed for $C_{12}OazoOH$ (**E**) (compared **Figure 3 A** and **B** near the collapse). These aggregates were able to form mesoscopic-sized supramolecular assemblies having a regular molecular alignment with strong birefringence; hence, their aggregates may be detected directly using polarized light microscopy. It is known that E azobenzene derivatives have a high tendency to form face-to-face H-aggregates, both in bulk crystalline structures and in monolayers, as it has been demonstrated using a range of experimental techniques.[36, 37, 39-41] Interestingly, BAM experiments of $C_{12}OazoE_3OH$ **(Z) (Figure 3C),** showed worm-like shapes as surface pressure was increased.

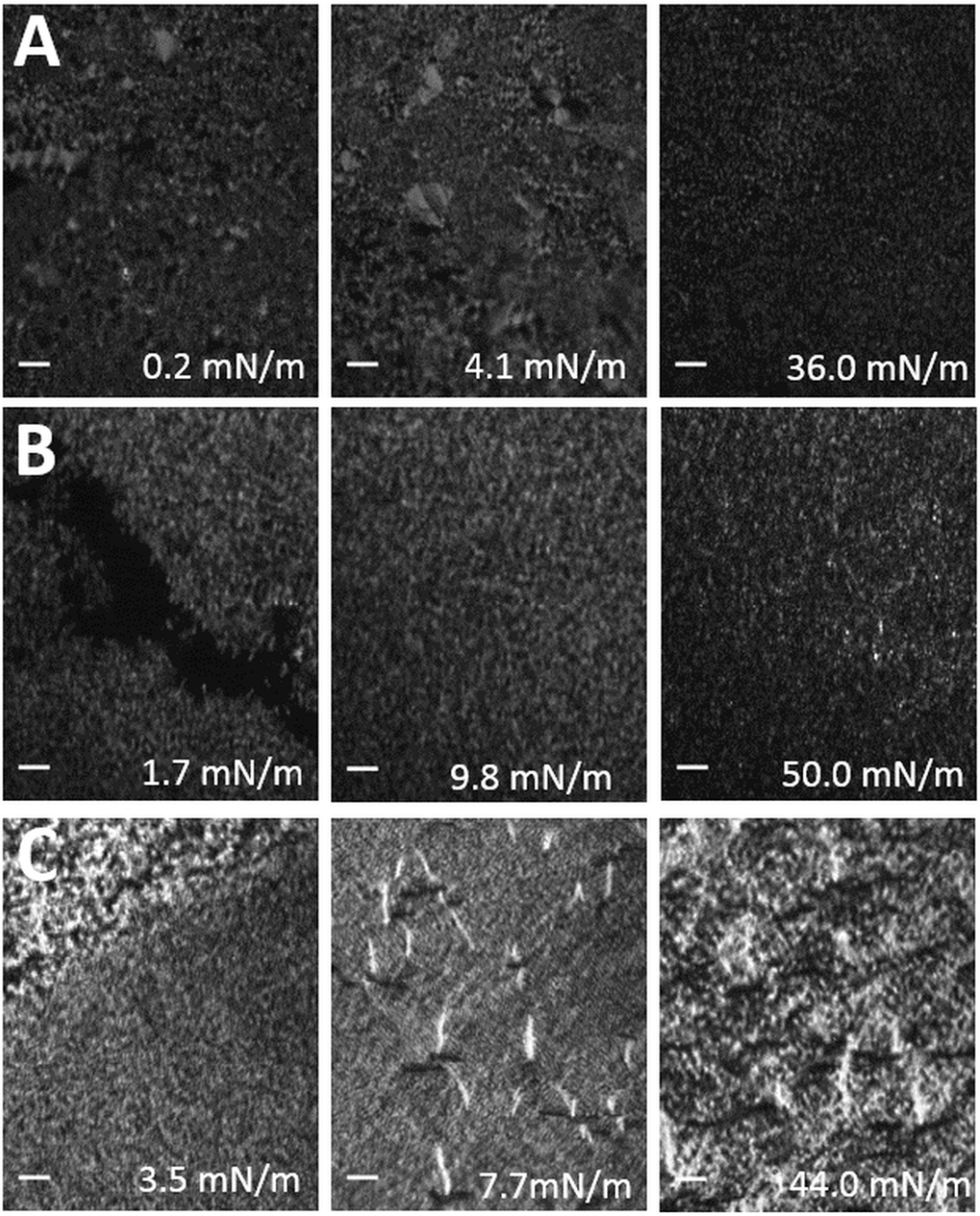

Figure 3. BAM micropictures at 13 ºC of**:** A) C_{12}OazoOH **(E)**, B) C_{12}OazoE$_3$OH **(E)**, C) C_{12}OazoE$_3$OH **(Z)**. Surface pressures are indicated in each picture (the complete sequence is presented in ESI: Fig S8, S9, S10, respectively). Scale bars correspond to 20 µm

These shapes were bright roads in vertical position and dark in horizontal position as a consequence of its differential interaction with polarized light. Therefore, it might be the same structure but at different polarization planes. In general, monolayer phases with tilted molecules often show long range tilt orientation order giving rise to optical anisotropy in the plane. The observed bright BAM reflectivity upon compression could be a result of the high tilted geometry of $C_{12}OazoE_3OH$ **(Z)** which is maintained near collapse. (**Figure 4**).

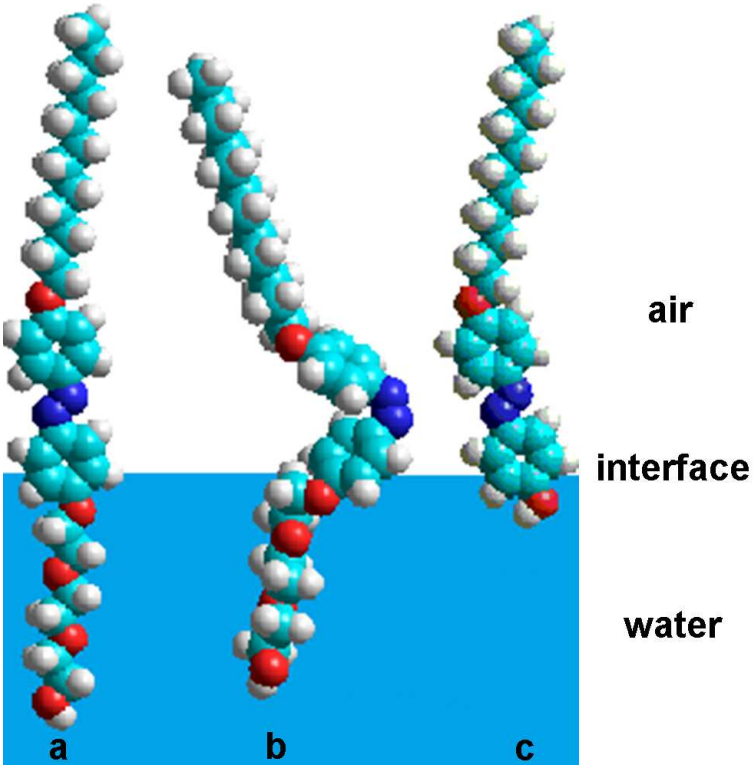

Figure 4. Proposed models near collapse of a) $C_{12}OazoE_3OH$ **(E),** b) $C_{12}OazoE_3OH$ **(Z)** and c) $C_{12}OazoOH$ **(E)** molecules at the interfase air/water**.** Atoms reference**:** red (Oxygen), light blue (Carbon), blue (Nitrogen), white (Hydrogen)

Photoisomerization at the interface. First, monolayers of $C_{12}OazoE_3OH$ **(E)** were kept at a surface pressure of 2 mN/m and 10 mN/m in independent experiments and then, both systems were allowed to equilibrate for several minutes. After that, the monolayers were illuminated by UV-light for 40

min. When UV-light irradiation was stopped, both systems were kept in darkness. A decrease in the MMA of 8 ± 1 and 6 ± 1 was detected, respectively (ESI, Fig. S11). The observed behavior has been previously reported for other azoamphiphiles. [29, 30] It has been explained considering that in general molecules of **E** azobenzenes possess a zero dipolar moment meanwhile **Z** isomers display an increase of around 4 Debye in many cases. [6] Thus, the increase of the molecular dipole moment in the **Z** configuration should increase their solubility in the subphase (aqueous solvent) and the loss of $C_{12}OazoE_3OH$ **(Z)** molecules would be reflected by a reduction of the monolayer area. Nevertheless this experiment showed that $C_{12}OazoE_3OH$ **(E)** monolayers could be disturbed by UV-light illumination.

Langmuir Monolayers of a Biomimetic Lipid Membrane and $C_{12}OazoE_3OH$. Lipoid s75^{TM} composed of 75% of phosphatidylcholine could be a suitable model of biological membrane because of its complexity.[31,42] For this reason, we envisaged that the evaluation of $C_{12}OazoE_3OH$ integrated in this membrane could be used as a proof of concept of the utility of $C_{12}OazoE_3OH$ as photoswitchable probe in real biomembranes. When Lipoid s75^{TM} was spread at the air/water interface, with or without 20 mol% of $C_{12}OazoE_3OH$ **(E)** or $C_{12}OazoE_3OH$ **(Z)**, the compression isotherm showed a smooth slope according to a LE behavior at low surface pressures (see inset in **Figure 5**). The beginning of a LE-LC transition is observed only for $C_{12}OazoE_3OH$ **(Z)** at about 12 mN/m. The compressibility modulus for pure Lipoid s75^{TM} was lower (~45 mN/m) than the values reached by monolayers formed by mixtures of Lipoid s75^{TM} and $C_{12}OazoE_3OH$ **(E)** or **(Z)** which were both similar (~70 mN/m) at high pressures (**Figure 5**). This increase showed that $C_{12}OazoE_3OH$ conferred to the membrane a more condensed character which was expected considering the molecular rigidity of the azoamphiphile and the solid- like character at the interface. Interestingly, below 20 mol % of $C_{12}OazoE_3OH$, the lipid did not show a significant variation of the interfacial behavior. Considering the complexity of the system, we decided to further evaluate

Lipoid s75^{TM} /$C_{12}OazoE_3OH$ in bulk in order to detect other changes on Lipoid s75^{TM} membrane promoted by the presence of $C_{12}OazoE_3OH$.

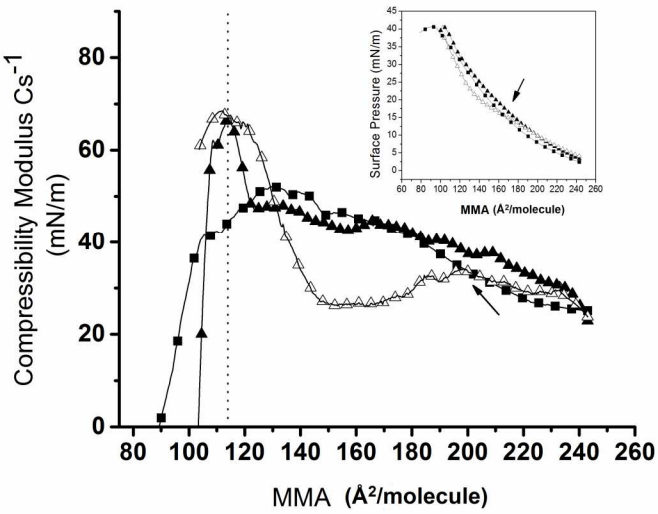

Figure 5. Compressibility modulus of a representative monolayer composed of Lipoid s75^{TM}: $C_{12}OazoE_3OH$ (**E**) (80:20 mol%) (▲), Lipoid s75^{TM}: $C_{12}OazoE_3OH$ (**Z**) (80:20 mol%) (△) and pure Lipoid s75^{TM} (■) as a function of surface molecular packing. The inset shows compression isotherms which were used to calculate compressibility modulus. The arrows indicate the beginning of the more condensed phase. The curves shown are chosen from a set of duplicates that differed by less than 2 Å^2/molecule.

Photoisomerization of Vesicular Membranes. Vesicular membranes of Lipoid s75^{TM} alone and with $C_{12}OazoE_3$ **(E)** were obtained by evaporation-hydration method.[43, 44] After UV illumination of Lipoid s75^{TM}: $C_{12}OazoE_3OH$ **(E)** mixture in water, a color change from yellow to orange was observed (as detected when pure $C_{12}OazoE_3OH$ **(E)** was illuminated in chloroform). Photoisomerization of Lipoid s75^{TM}: $C_{12}OazoE_3OH$ proceed smoothly as observed for pure $C_{12}OazoE_3OH$ in chloroform (compare Figures 1 and 6). The position of the absorption maxima of π- π* transition of $C_{12}OazoE_3OH$ **(E)** centered in 358 nm is characteristic of (E) monomer, showing

that the azoamphiphile is well mixed among the lipids, inhibiting the formation of H aggregates in the biomembrane and allowing complete photoisomerization.[14, 45]

After UV illumination π- π* transition maxima is centered in 323 nm and the n- π*transition at 450 nm increases which corresponds to (Z) isomer. It is possible to estimate a 10:90 pss, which is much higher than those reported previously for a ionic pseudoglyceryl single chain azobenzene lipid integrated in a phospholipid vesicular membrane (35:65 pss).[46]

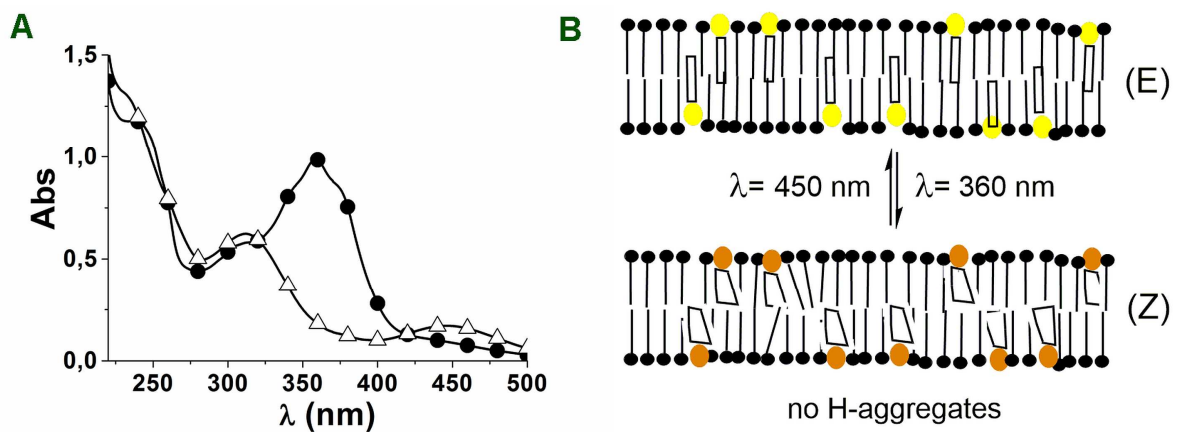

Figure 6. A) UV-Vis spectra of $C_{12}OazoE_3OH$ before (●) and after (△) UV-light illumination in the vesicular membrane. B) Schematic representation of $C_{12}OazoE_3OH$ (E) in yellow and $C_{12}OazoE_3OH$ (Z) in orange integrated in the biomembrane.

Physical changes of a biomimetic membrane promoted by $C_{12}OazoE_3OH$. The Mutilamellar vesicular dispersions described above were observed in a polarizer optical microscope (POM) under crossed polarizers. Because of the complexity of the whole system, all POM experiments were performed at 25°C where lamellar phases of PC are favored.[47, 48] In fact, dispersion of Lipoid s75™ pure in water formed lyotropic myelin figures, which are multilamellar tubular microstructures (**Figure 7A**).[49] On the other hand, mixtures of $C_{12}OazoE_3OH$ either in **(E)** or **(Z)** and Lipoid s75™ showed two different but very complex lyotropic pattern, which resembled laminar phase. Importantly, the presence of $C_{12}OazoE_3OH$ in the mixture of Lipoid s75™ inhibited the formation

of myelin figures (**Figure 7B and 7C**).[50] It seems that the incorporation of $C_{12}OazoE_3OH$ among Lipoid s75™ breaks the tubular myelin structure towards the formation of little folded sheets called lamellae, which in some cases twist themselves into a circular arrangement called spherulites.[51, 52]

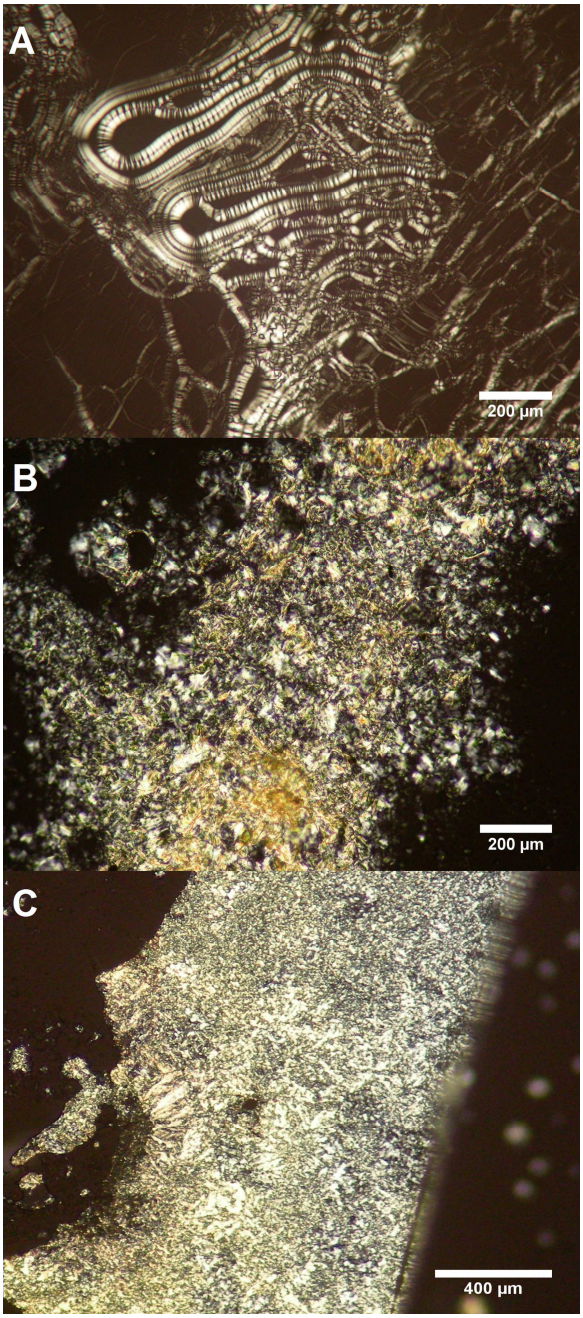

Figure 7. POM micrograph (crossed polarizers) of vesicular membrane dispersions at 25°C of A) Lipoid s75 ™, B) mixture of Lipoid s75 ™ / $C_{12}OazoE_3OH$ (E) (80:20 mol%), C) mixture of Lipoid s75 ™ / $C_{12}OazoE_3OH$ (Z) (80:20 mol%). The concentration of all dispersions was 2.8 mg/ml.

Differential scanning calorimetry (DSC) experiments of multilamellar vesicular membranes of Lipoid s75™ alone showed a non-cooperative transition temperature (Tm) of ~ 58°C (**Figure 8A**) which in the presence of 20 mol % $C_{12}OazoE_3OH$ **(E)**, increased to 100 °C (**Figure 8C**), showing that $C_{12}OazoE_3OH$ **(E)** transferred its structural rigidity to the lipid environment**.** After UV-illumination Tm shifted to ~ 80 °C (**Figure 8D**), showing that $C_{12}OazoE_3OH$ **(Z)** induces a decrease on the thermal transition temperature because of its bent molecular structure. Probably, both $C_{12}OazoE_3OH$ isomers are inserted with its large hydroxyl head close to the polar head of the lipids and partly immobilize those regions of the hydrocarbon chains closest to the polar head groups, similar to the known cholesterol interaction with lipids. In addition, the broad DSC peaks does not allow an accurate calculation of thermodynamics parameters, however they evidenced that the transition is non-cooperative, which it was expected for complex systems like Lipoid biomimetic membranes.[53] In addition, recently it was described that in the tilted gel phase, complex shapes can form spontaneously even in a membrane containing only a single lipid component leading non-cooperative transitions.[54]

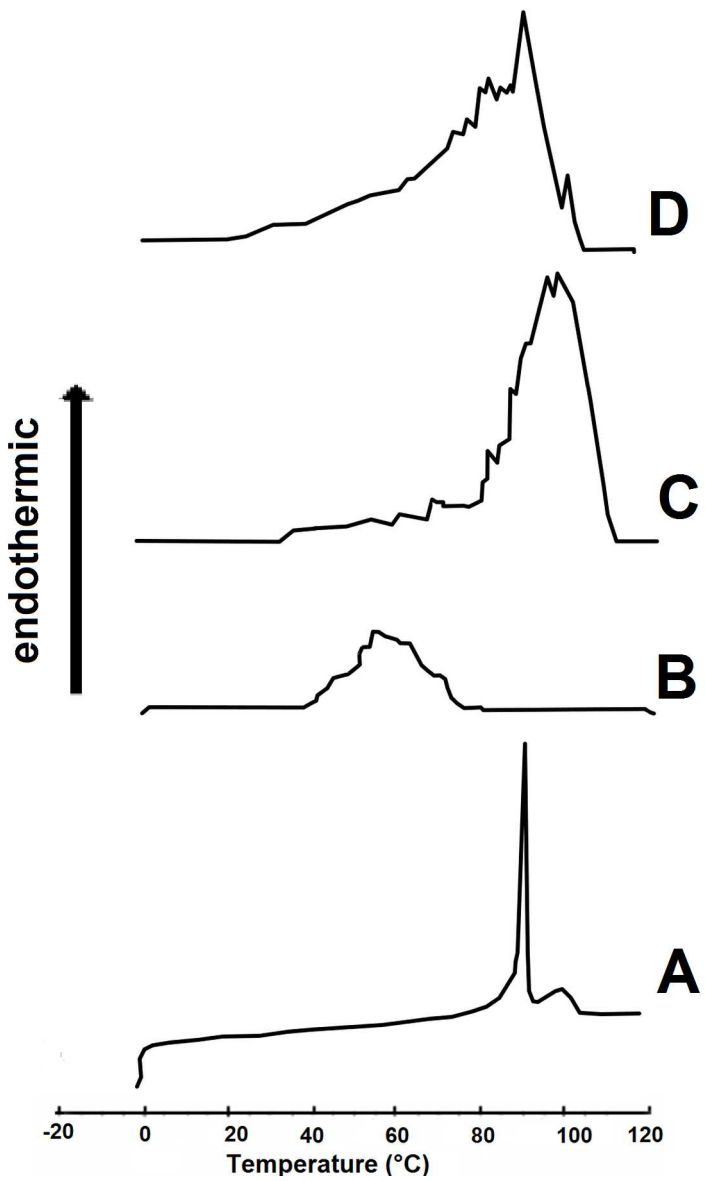

Figure 8. From bottom to top: DSC thermograms are shown A) solid $C_{12}OazoE_3OH$*, B) multilamellar vesicular dispersion of Lipoid s75 ™; C) multilamellar vesicular dispersion of Lipoid s75™: $C_{12}OazoE_3OH$ (E) mixture (80:20 mol%); D) multilamellar vesicular dispersion of Lipoid s75 ™: $C_{12}OazoE_3OH$ (Z) mixture (80:20 mol%). Concentration of all dispersion was 2.8 mg/ml.* Cr-SmC at 91.67°C (ΔH= 88.10 J g^{-1}) SmC-PI at 107.28 °C (ΔH= 33.77 J g^{-1}). The thermotropic behavior of pure $C_{12}OazoE_3OH$ is not described here.

Gibbs Monolayers. If $C_{12}OazoE_3OH$ will be used as remote photo-control molecule in real membranes, it would be capable to penetrate a highly compact monolayer. To this aim, Gibbs monolayers of (E) and (Z) $C_{12}OazoE_3OH$ were obtained on a bare surface to evaluate the increase on surface pressure when the corresponding $C_{12}OazoE_3OH$ isomer was injected under the subphase.[25] The pressures reached were ~ 25 mN/m for $C_{12}OazoE_3OH$ **(E)** and 20 mN/m for $C_{12}OazoE_3OH$ **(Z)** at concentration of 3.20 μM and 6.39 μM, respectively (**Figure 9A**). Then, the penetration behavior of $C_{12}OazoE_3OH$ **(E)** and $C_{12}OazoE_3OH$ **(Z)** into a preformed Lipoid s75™ monolayer showed that both isomers were able to penetrate the lipid monolayer for all initial surface pressures tested (**figure 9B).** The values plotted are for separated monolayers of different initial surface pressures obtained by the addition of $C_{12}OazoE_3OH$ **(E)** and $C_{12}OazoE_3OH$ **(Z),** respectively. Marsh has shown that, the best correspondence with various bilayer properties of pure lipids and biological membranes is obtained for monolayers at surface pressure of 30-35 mN/m.[55] More recently, a correspondence between bilayers and monolayers of pure lipids were obtain by multiphoton excitation fluorescence microscopy.[56] These authors reported that monolayer-bilayer correspondence occurs when the lateral pressure of the monolayer is 26-28 mN/m and 28-31 mN/m for DOPC and DPPC, respectively. Our experiments showed that, $C_{12}OazoE_3OH$ **(E)** penetrates the lipid monolayer to an extrapolated maximal pressure of ~ 37 mN/m, and $C_{12}OazoE_3OH$ **(Z)** reaches the highest cut off value at ~ 43 mN/m. The obtained extrapolated maximal values are in the range of other penetrating molecules, like δ-lysin (33 mN/m) and melitin (43 mN/m) and their interaction with real reconstituted biomembrane like sheep erythrocyte lipids.[57]

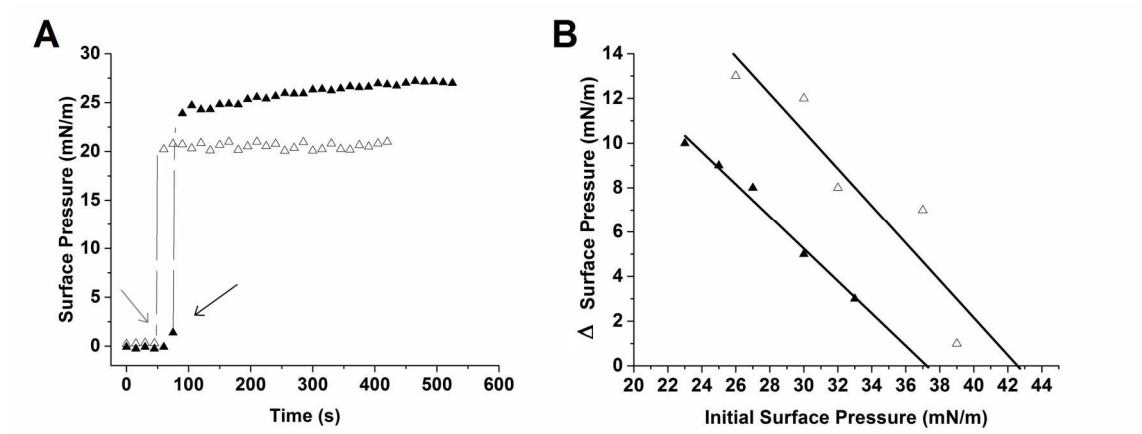

Figure 9: A) Gibbs monolayers of $C_{12}OazoE_3OH$ (E) (▲) and $C_{12}OazoE_3OH$ (Z) (△) formed by adsorption to a bare air/saline solution subphase. The curves are representative of three experiments developed in independent runs. The arrows indicate the time of $C_{12}OazoE_3OH$ (E) (black) and $C_{12}OazoE_3OH$ (Z) (grey) injection into the subphase, respectively **B)** Penetration cutoff curves for $C_{12}OazoE_3OH$ (E) (▲) and $C_{12}OazoE_3OH$ (Z) (△)into Lipoid s75^{TM} monolayers at different initial surface pressure (mN/m). Results represent the average of two independent experiments. Final subphase concentration was 3.20 μM $C_{12}OazoE_3OH$ (E) for and 6.39 μM for $C_{12}OazoE_3OH$ (Z).

It had been previously reported that the penetration ability of the amphiphiles depends on the aggregate size.[58, 59] Dynamic light scattering (DLS) experiments of $C_{12}OazoE_3OH$ (Z) in water showed that it was composed of one population of around 110 ± 50 nm of diameter, meanwhile $C_{12}OazoE_3OH$ (E) was composed of two population one of around 110 ± 20 nm and a second around 450 ±50 nm at room temperature (ESI, Fig. S12). This experiments suggest that $C_{12}OazoE_3OH$ (Z) molecules forms aggregates smaller than those of the $C_{12}OazoE_3OH$ **(E)** at the concentration tested and, thus, the subphase-surface equilibrium may be improved. The high cut off values obtained showed that $C_{12}OazoE_3OH$ might potentially penetrate a cell membrane.

CONCLUSION:

In conclusion, we provided experimental evidence that $C_{12}OazoE_3OH$ is a suitable optical controlled molecule. The supramolecular organization of pure $C_{12}OazoE_3OH$ at the interface is complex and it will be further studied by Langmuir-Blodgett films. $C_{12}OazoE_3OH$ was well integrated in a complex biomembrane model, like Lipoid s75^{TM}. The collapse surface pressure was similar (40 mN/m) for the biomembrane alone or mixtures with both $C_{12}OazoE_3OH$ isomers (20 mol%) however, a 25 mN/m increase of Cs^{-1} was detected in the presence of $C_{12}OazoE_3OH$, showing that the lipid membrane exhibits a more condensed character. Importantly, in the complex lipid mixture E→Z photoisomerization of $C_{12}OazoE_3OH$ proceeded smoothly depending on light conditions. It appears that the cross-sectional area of the hydroxyl triethylenglycol head of $C_{12}OazoE_3OH$ may inhibit azobenzene H aggregates formation in the model biomembrane. Because of that, the tails conformation change due to photoisomerization is transferred efficiently to the lipid membrane, photo-modulating the lipid physical properties. DSC and POM experiments showed that the E→Z photoisomerization in the lipid mixture induced thermal and morphological changes towards a more rigid system depending on light illumination, as observed by Langmuir monolayers. Probably, both $C_{12}OazoE_3OH$ isomers are inserted with its large hydroxyl head close to the polar head of the lipids and partly immobilize those regions of the hydrocarbon chains closest to the polar head groups, similar to cholesterol. A better understanding of this behavior will require the evaluation of $C_{12}OazoE_3OH$ with pure lipids. Finally, both $C_{12}OazoE_3OH$ (**E**) and (**Z**) isomers were able to penetrate a highly packing biomembrane, showing their potential as external probes in real systems. Further experiments are currently under progress to translate the use of $C_{12}OazoE_3OH$ to photo-control the translocation of other molecules through lipid membranes. [60]

AUTHOR INFORMATION

Corresponding Author

*E-mail: veronica.dodero@uns.edu.ar

Present Addresses

† Universität Bielefeld, Fakultät für Chemie, Organishe Chemie, Univeristätsstr. 25, 33615 Bielefeld, Germany, e-mail: veronica.dodero@uni-bielefeld.de

Author Contributions

The manuscript was written through contributions of all authors. All authors have given approval to the final version of the manuscript. ‡These authors contributed equally.

Acknowledgments

This work was supported mainly by UNS-PGI (Universidad Nacional del Sur), Secretary of Science and Technology of Universidad Nacional de Córdoba (SECyT-UNC), CONICET PIP 2014-2016 (National Scientific and Technical Research Council) and ANCyPT PICT-PRH 2010-2013 and PICT 2014-1627 (National Agency for Promotion of Science and Technology) Argentinian Research grants. M. A. S and L. A: B. are also grateful for their CONICET fellowship. B.M. and M.L.F. are Career Investigators of CONICET-UNC. V. I. D. and L. A. B. thank Prof. H Ritacco for monolayers reproducibility experiments. V. I. D. thanks Prof. N. Sewald from Fakultät Chemie, Universität Bielefeld for his support and J. L. Mascareñas for Mass Analysis. V.I.D acknowledges her Alexander von Humboldt Foundation fellowship (HERMES).

SUPPORTING INFORMATION Structural Characterization of $C_{12}OazoE_3OH$: ^{1}H-, ^{13} C-NMR Spectra, FAB spectra, Elemental Composition, Photo-conversion spectra, additional Langmuir monolayers and BAM experiments of $C_{12}OazoE_3OH$, DLS experiments of $C_{12}OazoE_3OH$.

REFERENCES:

(1) Whitesides, G. M. The 'Right' Size in Nanobiotechnology. *Nat. Biotechnolog.* **2003**, *21*, 1161-1165.

(2) Lehn, J. M. Toward Complex Matter: Supramolecular Chemistry and Self-Organization. *Proc. Natl. Acad. Sci. U. S. A.* **2002**, *99*, 4763-4768.

(3) Menger, F. M.; Gabrielson, K. D. Cytomimetic Organic Chemistry: Early Developments. *Angew. Chem., Int. Ed.* **1995**, *34*, 2091-2106.

(4) Wu, Z.; Yan, Y.; Huang, J. Advanced Molecular Self-Assemblies Facilitated by Simple Molecules. *Langmuir* **2014**, *30*, 14375-14384.

(5) Molla, M. R.; Ghosh, S. Aqueous Self-Assembly of Chromophore-Conjugated Amphiphiles. *Phys. Chem. Chem. Phys.* **2014**, *16*, 26672-26683.

(6) Feringa, B. Photoswitchable Polypeptides. *In Molecular Switches*, (Ed. Feringa); Wiley-VCH, Verlag GmbH, 2001; pp. 399-437.

(7) El Garah, M.; Palmino, F.; Cherioux, F. Reversible Photoswitching of Azobenzene-Based Monolayers Physisorbed on a Mica Surface. *Langmuir* **2010**, *26*, 943-949.

(8) Gong, Y.; Jiao, T.; Hu, Q.; Cheng, N.; Xu, W.; Bi, Y.; Yu, L. Rational Design of Multiple-Stimulus-Responsive Materials via Supramolecular Self-Assembly. *J. Phys. Chem. C* **2015**, *119*, 16349-16357.

(9) Wang, Y.; Ma, N.; Wang, Z.; Zhang, X. Photocontrolled Reversible Supramolecular Assemblies of an Azobenzene-Containing Surfactant with Alpha-Cyclodextrin. *Angew. Chem., Int. Ed.* **2007**, *46*, 2823-2826.

(10) Kauscher, U.; Samanta, A.; Ravoo, B. J. Photoresponsive Vesicle Permeability Based on Intramolecular Host-Guest Inclusion. *Org. Biomol. Chem.* **2014**, *12*, 600-606.

(11) Mansfeld, F. M.; Feng, G.; Otto, S. Photo-Induced Molecular-Recognition-Mediated Adhesion of Giant Vesicles. *Org. Biomol. Chem.* **2009**, *7*, 4289-4295.

(12) Folgering, J. H. A.; Kuiper, J. M.; de Vries, A. H.; Engberts, J. B. F. N.; Poolman, B. Lipid-Mediated Light Activation of a Mechanosensitive Channel of Large Conductance. *Langmuir* **2004**, *20*, 6985-6987.

(13) Asano, T.; Okada, T. Thermal Z-E isomerization of azobenzenes. The pressure, Solvent, and Substituent Effects. *J. Org. Chem.* **1984**, *49*, 4387-4391.

(14) Whitten, D. G.; Chen, L.; Geiger, H. C.; Perlstein, J.; Song, X. Self-Assembly of Aromatic-Functionalized Amphiphiles: The Role and Consequences of Aromatic−Aromatic Noncovalent Interactions in Building Supramolecular Aggregates and Novel Assemblies. *J. Phys. Chem. B* **1998**, *102*, 10098-10111.

(15) Wu, S.; Niu, L.; Shen, J.; Zhang, Q.; Bubeck, C. Aggregation-Induced Reversible Thermochromism of Novel Azo Chromophore-Functionalized Polydiacetylene Cylindrical Micelles. *Macromolecules* **2009**, *42*, 362-367.

(16) Yang, L.; Takisawa, N.; Hayashita, T.; Shirahama, K. Colloid Chemical Characterization of the Photosurfactant 4-Ethylazobenzene 4'-(Oxyethyl)trimethylammonium Bromide. *J. Phys. Chem. B* **1995**, *99*, 8799-8803.

(17) Zou, J.; Tao, F.; Jiang, M. Optical Switching of Self-Assembly and Disassembly of Noncovalently Connected Amphiphiles. *Langmuir* **2007**, *23*, 12791-12794.

(18) Cui, Z. K.; Phoeung, T.; Rousseau, P. A.; Rydzek, G.; Zhang, Q.; Bazuin, C. G.; Lafleur, M. Nonphospholipid Fluid Liposomes with Switchable Photocontrolled Release. *Langmuir* **2014**, *30*, 10818-10825.

(19) Shang, T.; Smith, K. A.; Hatton, T. A. Self-assembly of a Nonionic Photoresponsive Surfactant Under Varying Irradiation Conditions: a Small-Angle Neutron Scattering and Cryo-TEM Study. *Langmuir* **2006**, *22*, 1436-1442.

(20) Trappmann, B.; Ludwig, K.; Radowski, M. R.; Shukla, A.; Mohr, A.; Rehage, H.; Bottcher, C.; Haag, R. A New Family of Nonionic Dendritic Amphiphiles Displaying Unexpected Packing Parameters in Micellar Assemblies. *J. Am. Chem. Soc.* **2010**, *132*, 11119-11124.

(21) Nachtigall, O.; Kördel, C.; Urner, L. H.; Haag, R. Photoresponsive Switches at Surfaces Based on Supramolecular Functionalization with Azobenzene–Oligoglycerol Conjugates. *Angew. Chem., Int. Ed.* **2014**, *53*, 9669-9673.

(22) Shang, T.; Smith, K. A.; Hatton, T. A. Photoresponsive Surfactants Exhibiting Unusually Large, Reversible Surface Tension Changes under Varying Illumination Conditions. *Langmuir* **2003**, *19*, 10764-10773.

(23) Kordel, C.; Popeney, C. S.; Haag, R. Photoresponsive Amphiphiles Based on Azobenzene-Dendritic Glycerol Conjugates Show Switchable Transport Behavior. *Chem. Commun.* **2011**, *47*, 6584-6586.

(24) Mikhailov, A. S.; Ertl, G. Nonequilibrium Structures in Condensed Systems. *Science* **1996**, *272*, 1596-1597.

(25) Maget-Dana, R. The Monolayer Technique: a Potent Tool for Studying the Interfacial Properties of Antimicrobial and Membrane-Lytic Peptides and their Interactions with Lipid Membranes. *Biochim. Biophys. Acta, Biomembr.* **1999**, *1462*, 109-140.

(26) Kaganer, V. M.; Möhwald, H.; Dutta, P. Structure and Phase Transitions in Langmuir Monolayers. *Rev. Mod. Phys.* **1999**, *71*, 779-819.

(27) Brezesinski, G.; Möhwald, H. Langmuir Monolayers to Study Interactions at Model Membrane Surfaces. *Adv. Colloid Interface Sci.* **2003**, *100–102*, 563-584.

(28) Pulido-Companys, A.; Ignes-Mullol, J. Thermodynamics and Mesoscopic Organisation in Langmuir Monolayers of an Azobenzene Derivative. *J. Colloid Interface Sci.* **2010**, *352*, 449-455.

(29) Crusats, J.; Albalat, R.; Claret, J.; Ignes-Mullol, J.; Sagues, F. Influence of Temperature and Composition on the Mesoscopic Textures of Azobenzene Langmuir Monolayers. *Langmuir* **2004**, *20*, 8668-8674.

(30) Pulido-Companys, A.; Albalat, R.; Garcia-Amoros, J.; Velasco, D.; Ignes-Mullol, J. Supramolecular Chiral Azobenzene Surfactants. *Langmuir* **2013**, *29*, 9635-9642.

(31) Gibis, M.; Rahn, N.; Weiss, J. Physical and Oxidative Stability of Uncoated and Chitosan-Coated Liposomes Containing Grape Seed Extract. *Pharmaceutics* **2013**, *5*, 421-433.

(32) Gaines, G. L, *Insoluble monolayers at liquid-gas interfaces*. Interscience Publishers: New York, U.S.A, 1966.

(33) Fanani, M. L.; Maggio, B. Liquid-liquid Domain Miscibility Driven by Composition and Domain Thickness Mismatch in Ternary Lipid Monolayers. *J. Phys. Chem. B* **2011**, *115*, 41-49.

(34) Israelachvili, J. N.; Mitchell, D. J.; Ninham, B. W. Theory of Self-Assembly of Lipid Bilayers and Vesicles. *Biochim. Biophys. Acta* **1977**, *470*, 185-201.

(35) Seki, T.; Fukuchi, T.; Ichimura, K. Langmuir Monolayers of Azobenzene Derivative with a Urea Head Group. *Bull. Chem. Soc. Jpn.* **1998**, *71*, 2807-2816.

(36) Durbin, M. K.; Malik, A.; Richter, A. G.; Yu, C. J.; Eisenhower, R.; Dutta, P. Ordered Phases in Langmuir Monolayers of an Azobenzene Derivative. *Langmuir* **1998**, *14*, 899-903.

(37) Pedrosa, J.-M.; Romero, M. T. M.; Camacho, L.; Möbius, D. Organization of an Amphiphilic Azobenzene Derivative in Monolayers at the Air−Water Interface. *J. Phys. Chem. B* **2002**, *106*, 2583-2591.

(38) Rogez, D.; Benguigui, L. G.; Martinoty, P. Behavior of the Layer Compression Elastic Modulus Near, Above, and Below a Smectic C-Hexatic I Critical Point in Binary Mixtures. *Eur. Phys. J. E: Soft Matter Biol. Phys.* **2005**, *16*, 193-198.

(39) Xu, G.; Okuyama, K.; Shimomura, M. Crystal Structures of H-Aggregate of Azobenzene-Containing Amphiphiles, C6AzoC8N+ Br− and C8AzoC10N+ Br−. *Mol. Cryst. Liq. Cryst. Sci. Technol., Sect. A* **1992**, *213*, 105-115.

(40) Kawai, T.; Umemura, J.; Takenaka, T. UV Absorption Spectra of Azobenzene-Containing Long-Chain Fatty Acids and their Barium Salts in Spread Monolayers and Langmuir-Blodgett Films. *Langmuir* **1989**, *5*, 1378-1383.

(41) Maack, J.; Ahuja, R. C.; Tachibana, H. Resonant and Nonresonant Investigations of Amphiphilic Azobenzene Derivatives in Solution and in Monolayers at the Air/Water Interface. *J. Phys. Chem.* **1995,** *99*, 9210-9220.

(42) Delmas, T.; Couffin, A. C.; Bayle, P. A.; de Crecy, F.; Neumann, E.; Vinet, F.; Bardet, M.; Bibette, J.; Texier, I. Preparation and Characterization of Highly Stable Lipid Nanoparticles with Amorphous Core of Tuneable Viscosity. *J. Colloid Interface Sci.* **2011**, *360*, 471-481.

(43) Chapman, D. Phase Transitions and Fluidity Characteristics of Lipids and Cell Membranes. *Q. Rev. Biophys.* **1975**, *8*, 185-235.

(44) Lasic, D. D. Chapter 10 - Applications of Liposomes. In *Handbook of Biological Physics*, Lipowsky, R.; Sackmann, E., Eds. North-Holland: 1995; Vol. Volume 1, pp 491-519.

(45) Kuiper, J. M.; Engberts, J. B. H-Aggregation of Azobenzene-Substituted Amphiphiles in Vesicular Membranes. *Langmuir* **2004**, *20*, 1152-1160.

(46) Moss, R. A.; Jiang, W. Cis/Trans Isomerization in Azobenzene-Chain Liposomes. *Langmuir* **1995**, *11*, 4217-4221.

(47) Luzzati, V.; Gulik-Krzywicki, T.; Tardieu, A. Polymorphism of Lecithins. *Nature* **1968**, *218*, 1031-1034.

(48) Tardieu, A; Luzzati, V.; Reman, F.C. Structure and Polymorphism of the Hydrocarbon Chains of Lipids: A Study of Lecithin-Water Phases. *J. Mol. Biol*. **1973**, *75*, 711-733.

(49) Sakurai, I.; Kawamura, Y., Growth Mechanism of Myelin Figures of Phosphatidylcholine. *Biochim. Biophys. Acta* **1984**, *777*, 347-351.

(50) Peddireddy, K.; Kumar, P.; Thutupalli, S.; Herminghaus, S.; Bahr, C. Myelin Structures Formed by Thermotropic Smectic Liquid Crystals. *Langmuir* **2013**, *29*, 15682-15688.

(51) Simarda, P.; Hoaraub, D.; Khalida, M. N.; Rouxa, E.; Leroux, J. C. Preparation and in Vivo Evaluation of PEGylated Spherulite Formulations. *Biochim. Biophys. Acta* **2005***, 1715*, 37-48.

(52) Lugito, G.; Woo, E. M. Lamellar Assembly Corresponding to Transitions of Positively to Negatively Birefringent Spherulites in Poly(ethylene Adipate) with Phenoxy. *Colloid Polym. Sci*. **2013**, *291*, 817-826.

(53) McElhoney, R. The Use of Differential Scanning Calorimetry and Differential Thermal Analysis in Studies of Model and Biological Membranes. *Chem. Phys. Lipids* **1982**, *30*, 229-259.

(54) Hirst, L. S.; Ossowski, A.; Fraser, M.; Geng, J.; Selinger, J. V.; Selinger, R. L. B. Morphology Transition in Lipid Vesicles due to in-Plane Order and Topological Defects. *Proc. Natl. Acad. Sci. U. S. A.* **2013**, *110*, 3242–3247.

(55) Marsh, D. Lateral Pressure in Membranes. *Biochim. Biophys. Acta* **1996**, *1286*, 183-223.

(56) Brewer, J.; De la Serna, J. B.; Wagner, K.; Bagatolli, L. A. Multiphoton Excitation Fluorescence Microscopy in Planar Membrane Systems. *Biochim. Biophys. Acta* **2010**, *1798*, 1301–1308.

(57) Bhakoo, M.; Birkbeck, T. H.; Freer, J. H. Interaction of Staphylococcus Aureus Delta.-Lysin with Phospholipid Monolayers. *Biochemistry* **1982**, *21*, 6879-6883.

(58) Mottola, M.; Wilke, N.; Benedini, L.; Oliveira, R. G.; Fanani, M. L. Ascorbyl Palmitate Interaction with Phospholipid Monolayers: Electrostatic and Rheological Preponderancy. *Biochim. Biophys. Acta* **2013**, *1828*, 2496-2505.

(59) Benedini, L.; Fanani, M. L.; Maggio, B.; Wilke, N.; Messina, P.; Palma, S.; Schulz, P. Surface Phase Behavior and Domain Topography of Ascorbyl Palmitate Monolayers. *Langmuir* **2011**, *27*, 10914-1099.

(60) Sebai, S. C.; Milioni, D.; Walrant, A.; Alves, I. D.; Sagan, S.; Huin, C.; Auvray, L.; Massotte, D.; Cribier, S.; Tribet, C. Photocontrol of the Translocation of Molecules, Peptides, and Quantum Dots through Cell and Lipid Membranes Doped with Azobenzene Copolymers. *Angew. Chem., Int. Ed.* **2012,** *51*, 2132-2136.

TOC

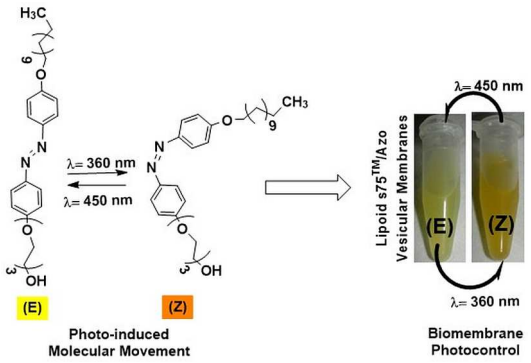
H3C
CH3
λ= 360 nm
λ= 450 nm
OH
(E)
(Z)
Photo-induced
Molecular Movement
λ= 450 nm
Lipoid s75TM/Azo
Vesicular Membranes
(E)
(Z)
λ= 360 nm
Biomembrane
Photocontrol